Structural and spectroscopic studies of $La_2Ce_2O_7$: Disordered fluorite versus pyrochlore structure

Emily Reynolds, Peter E. R. Blanchard, Qingdi Zhou, and Brendan J. Kennedy*
School of Chemistry, The University of Sydney, Sydney, NSW 2006, Australia

Zhaoming Zhang
Institute of Materials Engineering, Australian Nuclear Science and Technology Organisation, Lucas Heights, New South Wales 2234, Australia

Ling-Yun Jang
Facility Utilization Group, Experiment Facility Division, National Synchrotron Radiation Research Center, Hsinchu 300, Taiwan
(Received 15 December 2011; published 24 April 2012)

We present the neutron and synchrotron x-ray diffraction and Ce L_3-edge x-ray absorption near-edge structure results for polycrystalline $La_2Ce_2O_7$. We have found that this compound adopts a disordered defect fluorite structure with diffuse features evident in the neutron-diffraction pattern indicative of anion disorder. Our experimental results are discussed in the context of a recent theoretical paper on this material.

DOI: 10.1103/PhysRevB.85.132101 PACS number(s): 61.66.−f, 61.05.cp, 61.05.fg

I. INTRODUCTION

Lanthanum containing pyrochlores are of considerable interest due to their potential applications as an ionic conductor in solid oxide fuel cells,[1] as thermal barrier coatings for high-temperature applications[2,3] or as hosts for the storage of radioactive waste.[4,5] Despite this interest, there remains uncertainty regarding the precise structure of many examples with $La_2Ce_2O_7$ being the case at point. Some authors describe the structure of $La_2Ce_2O_7$ as a disordered defect fluorite ($La_{0.5}Ce_{0.5}O_{1.75}$)[6] and others as a pyrochlore.[7] There are reports of phase separation in mixed La-Ce fluorites $La_xCe_{1-x}O_{(2-x/2)}$ around $x = 0.5$ with the phases being sensitive to the thermal treatment of the samples.[8–10] Defects can change the thermodynamic stability of materials and can control many of their physical, chemical, and electronic properties. Understanding and controlling defect formation in complex structures is an important step for the rational development of advanced materials. The $A_2B_2O_7$ pyrochlore structure can be derived from the AO_2 fluorite structure by ordering of the vacant anion site and the two cations.[11] The general formula of oxide pyrochlores is often written as $A_2B_2O_6O'$ to distinguish the two different anion sites with O occupying the 48*f* Wykoff sites at (x,1/8,1/8) (in space group $Fd\bar{3}m$) and O′ the 8*b* sites at (3/8,3/8,3/8). The two cations occupy special positions with the larger *A*-type cation at 16*d* ($\frac{1}{2},\frac{1}{2},\frac{1}{2}$) and the smaller *B* cation at 16*c* (0,0,0). Hence, the structure is described by the cubic lattice parameter and the positional parameter x for O. In this description, the 8*a* site at (1/8,1/8,1/8) is unoccupied. In the $(A/B)O_{2-x}$ anion-deficient fluorite structure (space group $Fm\bar{3}m$), the two cations are disordered at the 4*a* site (0,0,0), and the anions occupy the 8*c* site at ($\frac{1}{4},\frac{1}{4},\frac{1}{4}$).

A large number of cation pairs form the pyrochlore structure with the ordering of the two cations being dependent on the size and charge difference between them. Empirical evidence suggests that, for 3 + /4 + oxides, the pyrochlore structure is favored where the ratio of cation sizes is $r_A/r_B > 1.42$.[11,12] At lower values, the disordered fluorite structure is expected to be more stable. In $La_2Ce_2O_7$, the ionic radii of eight-coordinate La^{3+} is 1.16 Å, while that of six-coordinate Ce^{4+} is 0.87 Å,[13] giving $r_A/r_B = 1.33$, suggesting the fluorite structure should be favored.

Very recently, Vanpoucke *et al.*[14] investigated the structure of $La_2Ce_2O_7$ using *ab initio* density functional theory (DFT) calculations. These authors concluded that the pyrochlore structure is energetically favored over the fluorite and presented some x-ray diffraction (XRD) data to support this conclusion. Neutrons are expected to be a more sensitive probe than x-rays to the structure of $La_2Ce_2O_7$ as a consequence of both their greater sensitivity to the lighter oxygen anions and the significantly different neutron-scattering lengths of isoelectronic La^{3+} and Ce^{4+} (8.24 and 4.84 fm, respectively[15]). Nevertheless, the two previously reported neutron-diffraction studies of $La_2Ce_2O_7$ are in conflict. In their early neutron-diffraction experiments, Brisse and Knop[16] concluded that $La_2Ce_2O_7$ adopted a disordered defect fluorite structure rather than a pyrochlore one. More recently, Bea *et al.*[7] concluded that the structure was, in fact, pyrochlore, although it must be noted that the sample they studied contained numerous weak reflections from a second phase. Bea *et al.*[7] did not report any structural parameters for their proposed pyrochlore structure. Obtaining precise structures is often critical in understanding complex phenomena in pyrochlores.[17] Clearly, there is the need to establish the precise structure of $La_2Ce_2O_7$.

In the present Brief Report, we report the results of our high-resolution neutron and synchrotron x-ray diffraction studies and demonstrate our material to have a cubic fluorite rather than a pyrochlore structure. X-ray absorption measurements confirm that Ce is tetravalent and support the conclusion, from the diffraction studies, that the local environment of Ce is not six coordinate. Evidence for mobility of the anions is also presented.

II. EXPERIMENT

Approximately 5 g of $La_2Ce_2O_7$ were synthesized using the method described by Brisse and Knop.[16] Stoichiometric amounts of La_2O_3 (Sigma-Aldrich, 99.99%) and CeO_2

(Sigma-Aldrich, 99.999%) were dissolved separately in 40-ml 15-M nitric acid for La_2O_3 and 500-ml 15-M nitric acid with 110 ml 30% weight-by-volume ratio of hydrogen peroxide for CeO_2. Note the CeO_2 did not dissolve completely. The two solutions were mixed in a 750-ml beaker and were brought to boil, at which time, 200 ml of a hot 20% oxalic acid solution was added. The mixture was taken to dryness under a lamp. The resulting cream-colored oxalate powder was heated at 600 °C for 1 h, was ground, was pressed into a pellet, and was heated at 950 °C for 4 h and then 1000 °C for 36 h. The pellet was reground, was repressed, and was heated at 1350 °C for 9 h and finally, at 1400 °C for 48 h. All heating was conducted in a muffle furnace in air.

The sample was sealed in a 9-mm diameter vanadium can for neutron powder-diffraction measurements; data were obtained using the high-resolution powder diffractometer Echidna at ANSTO's OPAL facility at Lucas Heights.[18] The wavelength of the incident neutrons, obtained using a Ge 335 monochromator, was 1.622 Å as determined using a National Institute of Standards and Technology (NIST) SRM676 Al_2O_3 standard. This instrument has a maximum d-spacing resolution of $\Delta d/d \sim 1 \times 10^{-3}$. Synchrotron x-ray powder diffraction data were collected from samples loaded into a 0.3-mm capillary over the angular range of $5 < 2\theta < 85°$ using x rays of wavelength 0.82465 Å, estimated using NIST SRM660a LaB_6, on the powder diffractometer at the BL-10 beamline of the Australian Synchrotron.[19]

The structure was refined using the Rietveld method as implemented in the program RIETICA.[20] The peak shapes were modeled using a pseudo-Voigt function. The zero correction, scale factor, half width parameters (u,v,w), lattice parameters, positional coordinates, and isotropic atomic displacement parameters were varied during the refinement. The neutron-scattering lengths of La, Ce, and O used in the refinements were 8.24, 4.84, and 5.803 fm, respectively.[15]

X-ray absorption near-edge structure (XANES) analysis was carried out on beamline 16A1 at the National Synchrotron Radiation Research Center (NSRRC) in Hsinchu, Taiwan.[21] The Ce L_3-edge spectra were obtained from $La_2Ce_2O_7$ and three Ce standards (CeO_2, $SrCeO_3$, and $CeAlO_3$) in the fluorescence mode using a Lytle detector from powder samples dispersed on Kapton tape. Energy steps as small as 0.2 eV were employed near the absorption edges with a counting time of 2 s per step. The spectra were normalized to the incident photon current. The energy scale was calibrated using the K edge of a pure Cr foil at 5989.2 eV.

III. RESULTS AND DISCUSSION

The radius ratio of $La_2Ce_2O_7$ $r_A/r_B = 1.33$ suggests that it should adopt a defect fluorite structure,[12] and the early neutron-diffraction study of Brisse and Knop[16] supports this conclusion. A synchrotron x-ray diffraction pattern of $La_2Ce_2O_7$, illustrated in Fig. 1, provides no evidence for any superlattice reflections indicative of a pyrochlore structure. In particular, there is no evidence for intensity at reflections, such as (311), (331), or (511) that are diagnostic of a pyrochlore structure. These reflections were clearly evident in data of pyrochlores, such as $La_2Zr_2O_7$. There was no evidence in the synchrotron x-ray profile for peak splitting indicative of phase

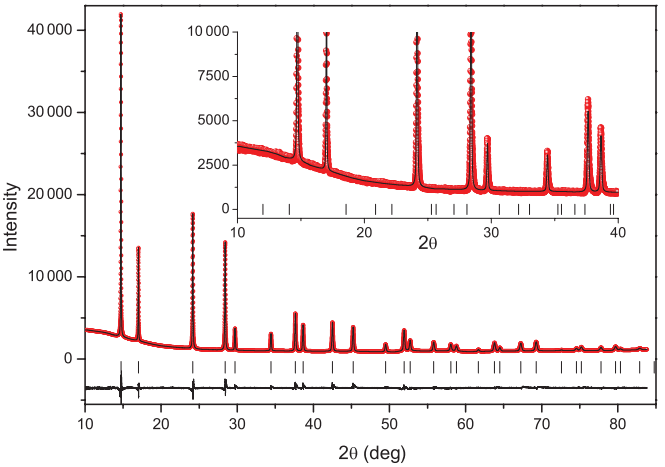

FIG. 1. (Color online) Rietveld refinement profile of the synchrotron XRD data of $La_2Ce_2O_7$. The symbols represent the observed data, and the solid line represents the fit to the fluorite model. The difference profile is shown below the Bragg reflection markers. The inset highlights the absence of any intensity indicative of a pyrochlore structure, and, in particular, no intensity is associated with the (311), (331), or (511) reflections. In the inset, only the positions of the extra peaks from the pyrochlore structure are indicated. The increase in intensity at low angles is due to air scatter.

separation, as observed by Ryan *et al.*[9] although the peaks did show slight asymmetry. Comparison of our Fig. 1 with Fig. 3 of Vanpoucke *et al.*[14] is informative, and our experimental data are clearly inconsistent with their calculated patterns. As noted above, neutron diffraction is expected to be a more sensitive probe in distinguishing between the pyrochlore and the fluorite structures, and Fig. 2 illustrates the results of our measurements. The only Bragg reflections observed in the neutron powder-diffraction (NPD) data were those indicative

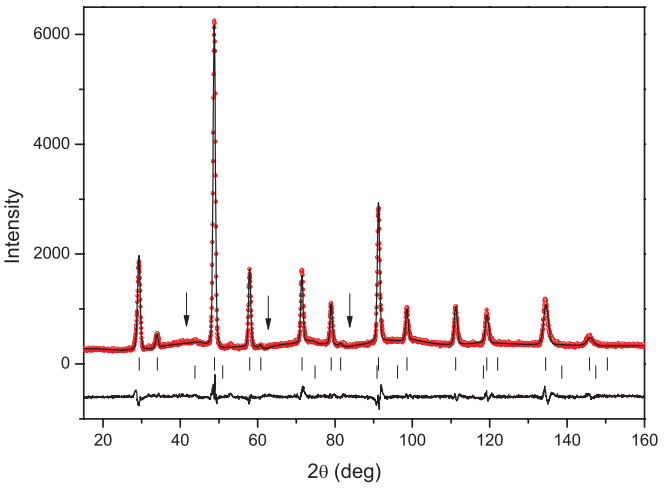

FIG. 2. (Color online) Rietveld refinement profile of neutron powder-diffraction data of $La_2Ce_2O_7$. The upper set of markers represents the fluorite phase, and the lower set represents a vanadium phase from the sample holder. The arrows indicate the positions of the strongest additional peaks that would be present if the structure was pyrochlore. Note the modulated diffuse background indicative of disorder.

of the fluorite-type structure, along with very weak peaks from the vanadium sample holder. No evidence is found for the pyrochlore phase. While heating the sample to 1400 °C at atmospheric pressure yields the fluorite, it is possible that the use of high-pressure synthesis conditions could alter the relative stability of the two phases. In the related $Ln_2Zr_2O_7$ (Ln = lanthanoid) series, the volume for the pyrochlore phase Vol_p is systematically larger than twice that of the fluorite phase Vol_f.[22] Since high pressures invariably favor the denser structure, the fluorite is expected to be stabilized by high-pressure synthetic methods.

Rietveld analysis was carried out assuming $Fm\bar{3}m$ symmetry (see Table I). Initially, we utilized a defect fluorite model where the Ce and La are disordered on the 4*a* (0,0,0) sites, and the oxygen partially occupies the 8*c* sites at $(\frac{1}{4},\frac{1}{4},\frac{1}{4})$. Refinement using this model rapidly converged with $\chi^2 = 1.62$. In these refinements, the atomic displacement parameter for the O atoms was noticeably larger than that for the mixed Ce/La cations, 3.96(4) vs 2.30(3) $\times$ 10^{-2} Å^2. The high U_{iso}(O) value indicates high dynamic motion and/or static positional disorder. To test the latter possibility, a model was created where some of the oxygen atoms were displaced from the 8*c* site and were distributed over the 8*c* and nearby 32*f* (*x*,*x*,*x*) positions ($x = \frac{1}{4} + \delta$).[23] This model, that describes the behavior of CeO_2,[23] failed to converge to chemically sensible values and was subsequently discounted.

A fit to a pyrochlore model in which the 8*a* (1/8,1/8,1/8) site was empty, calculated intensity where none was observed and yielded an unacceptably high $\chi^2 = 5.22$ value for the best fit with $x = 0.3686(4)$ and $a = 11.1301(5)$ Å. The refined *x* positional parameter is statistically shifted from 3/8, the equivalent position in an unrelaxed fluorite model, and toward the nominally vacant 8*a* site. Allowing the 8*a* site to be occupied resulted in a comparable fit to that obtained for the fluorite model with $\chi^2 = 1.57$ and $x = 0.3711(5)$. In this case, there is only minimal displacement of the anions on the 48*f* sites toward the 8*a* site as would be expected if this site was occupied. Within the precision of this refinement, the anion vacancies were uniformly distributed over the 48*f*, 8*a*, and 8*b* sites. These refinements verify the conclusion that the sample is fluorite, rather than pyrochlore.

A feature of the present neutron-diffraction pattern is the broad features, indicative of modulated diffuse scattering, evident in the background of the pattern. This background is similar to that seen in members of the series $Nd_{2-x}Ho_xZr_2O_7$ studied recently[22] and reflects the presence of disorder in the structure. It is worth noting that the background of a NPD pattern, measured for the pyrochlore $La_2Zr_2O_7$ under identical conditions, did not show any diffuse features. Given the neutron data for $La_2Ce_2O_7$ were obtained at ambient temperature, the structured background is not due to normal thermal diffuse scattering. That this diffuse background is not apparent in the x-ray diffraction profile and the refined displacement parameter U_{iso}(O) is significantly larger than U_{iso}(La/Ce) suggests a large diffusion coefficient of the oxide ions. The high U_{iso}(O) can be regarded as the structural indicator for high oxygen ion conduction in defect fluorites and corresponds to movement of oxygen ions across the unit cell. We note that the diffuse background is less developed than that observed for La-doped Bi_2O_3 by Verkerk *et al.*[24] suggesting an absence of appreciable short-range oxide-ion sublattice occupancy ordering.

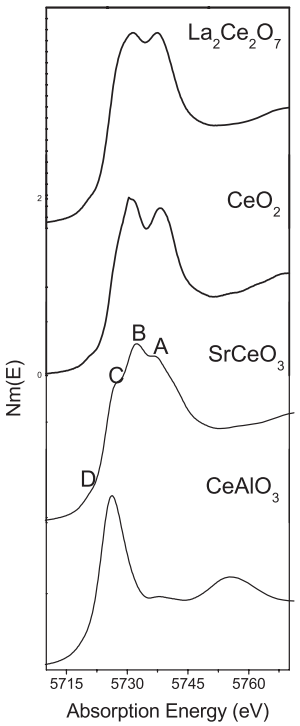

FIG. 3. Ce L_3-edge XANES spectra of $La_2Ce_2O_7$, CeO_2, $SrCeO_3$, and $CeAlO_3$.

Diffraction methods are a probe of long-range ordering of the ions, and the synchrotron x-ray and neutron powder-diffraction measurements clearly show the absence of any long-range pyrochlore-type ordering. It is, of course, possible that the local structure (coordination environment) of some Ce cations is significantly different from that of the long-range average structure, and this may drive the diffuse background seen in the neutron data. Consequently, a Ce L_3-edge XANES analysis was performed to provide further information on the oxidation state and local coordination environment of Ce. The Ce L_3-edge XANES spectrum of $La_2Ce_2O_7$ was compared to several Ce^{3+} and Ce^{4+} standards of various coordination environments (Fig. 3). It is well known that the line shape of the Ce L_3-edge XANES spectrum, which involves the dipole-allowed transition of $2p_{3/2}$ electrons into unoccupied

TABLE I. Structural parameters for $La_2Ce_2O_7$ from refinements against NPD data.

Space group	*a* (Å)	100 U_{iso}(La/Ce) (Å^2)	100 U_{iso}(O) (Å^2)	La/Ce-O (Å)	χ^2
$Fm\bar{3}m$	5.5657(1)	2.30(3)	3.96(4)	2.410 03(6)	1.62

$5d$ states, is highly sensitive to the oxidation state of Ce, as evident from the comparison of CeO_2 (Ce^{4+}) and $CeTiO_3$ (Ce^{3+}) (Ref. 25) or $Ce_{1/3}TaO_3$ (Ce^{3+}) (Ref. 26). Generally, four features (labeled A–D) are observed in the Ce^{4+} species compared to a single broad peak observed in Ce^{3+}. The single "white line" observed from the Ce^{3+} species is typical of a nearly pure $4f^1$ final state. Peaks A, B, and C are attributed to the $4f^0$, $4f^1$, and $4f^2$ final states of Ce^{4+}, respectively;[27] the $4f^1$ and $4f^2$ final states result from ligand-to-metal charge transfer. It has also been postulated that peak C is caused by Ce^{3+} impurities[28] or crystal-field splitting.[29] The weak preedge feature (labeled D) appears characteristic of Ce^{4+}, although there is some uncertainty regarding its origin.[28–30] Unsurprisingly, the line shape of the Ce L_3-edge XANES spectrum of $La_2Ce_2O_7$ is indicative of Ce^{4+}. What is remarkable is the obvious difference in the appearance of the Ce L_3-edge spectra between six-coordinate (e.g., $SrCeO_3$) and eight-coordinate (e.g., CeO_2) Ce^{4+} systems. It is currently not well understood how the ligand-to-metal charge-transfer final states are affected by the Ce^{4+} coordination environment (or, for that matter, how the covalency of Ce atoms change with coordination environment). Nevertheless, it is obvious that the Ce L_3-edge XANES spectrum of $La_2Ce_2O_7$ is much more similar to that of eight-coordinate CeO_2 than that of six-coordinate $SrCeO_3$, suggesting that the Ce ions have a local coordination greater than 6, and consequently, the local structure of the Ce in $La_2Ce_2O_7$ is fluoritelike. Recall that, although the average coordination of the Ce cations would be 7, as a consequence of the anion vacancies, the disorder of the vacancies would result in a range of coordination environments. Further studies are required to understand how the coordination environment influences the appearance of the Ce L_3-edge spectrum.

To summarize, a single phase sample of composition $La_2Ce_2O_7$ has been prepared using a maximum synthesis temperature of 1400 °C. Our experimental studies unequivocally demonstrate that $La_2Ce_2O_7$ adopts a disordered defect fluorite structure in which the Ce^{4+} cations are effectively seven coordinate. This is in conflict with the recent DFT calculations of Vanpoucke *et al.*,[14] and it is important to consider the origin of this difference, which may reflect assumptions in the theoretical calculation and experimental limitations. The DFT calculations are expected to identify a thermodynamic minimum, whereas, the experimental results reflect a balance between kinetic and thermodynamic contributions. In the disordered defect fluorite structure, there are a large number of configurations with different defect-defect distances,[31] and it is not clear how critical modeling the different defect formation energies is.[32] Changing experimental conditions can significantly alter the balance between the two structures as demonstrated for $Gd_2Zr_2O_7$ (Ref. 33) with the conditions employed in the present Brief Report expected to favor the thermodynamic rather than the kinetic product. It is unlikely that the observed fluorite structure represents a metastable phase that would transform to the pyrochlore if heated to near its melting point. In general, heating tends to increase the disorder in structures, and as observed in other systems, such as $Gd_2Zr_2O_7$, heating the pyrochlore leads to a transformation to the fluorite structure. Given the cation radius ratio for $La_2Ce_2O_7$, it is difficult to imagine experimental conditions that are likely to favor an ordered pyrochlore structure.

ACKNOWLEDGMENTS

This work was, in part, performed at the powder-diffraction beamline at the Australian Synchrotron with the assistance of Dr. Justin Kimpton. We thank Dr. Max Avdeev for collection of the neutron-diffraction data. B.J.K. acknowledges the support of the Australian Research Council for this work. The work performed at the NSRRC was supported by the Australian Synchrotron International Access Program.

*kennedyb@chem.usyd.edu.au

[1] H. Yamamura, H. Nishino, K. Kakinuma, and K. Nomura, J. Ceram. Soc. Jpn. **111**, 902 (2003).
[2] W. Ma, S. K. Gong, H. B. Xu, and X. Q. Cao, Surf. Coat. Technol. **200**, 5113 (2006).
[3] K. H. Kwak, B. C. Shim, S. M. Lee, Y. S. Oh, H. T. Kim, B. K. Jang, and S. Kim, Mater. Lett. **65**, 2937 (2011).
[4] K. B. Helean, A. Navrotsky, E. R. Vance, M. L. Carter, B. Ebbinghaus, O. Krikorian, J. Lian, L. M. Wang, and J. G. Catalano, J. Nucl. Mater. **303**, 226 (2002).
[5] J. Lian, K. B. Helean, B. J. Kennedy, L. M. Wang, A. Navrotsky, and R. C. Ewing, J. Phys. Chem. B **110**, 2343 (2006).
[6] X. Cao, R. Vassen, W. Fischer, F. Tietz, W. Jungen, and D. Stöver, Adv. Mater. **15**, 1438 (2003).
[7] J. S. Bae, W. K. Choo, and C. H. Lee, J. Eur. Ceram. Soc. **24**, 1291 (2004).
[8] B. C. Morris, W. R. Flavell, W. C. Mackrodt, and M. A. Morris, J. Mater. Chem. **3**, 1007 (1993).
[9] K. M. Ryan, J. P. McGrath, R. A. Farrell, W. M. O'Neill, C. J. Barnes, and M. A. Morris, J. Phys.: Condens. Matter **15**, L49 (2003).
[10] E. R. Andrievskaya, O. A. Kornienko, A. V. Sameljuk, and A. Sayir, J. Eur. Ceram. Soc. **31**, 1277 (2011).
[11] M. A. Subramanian, G. Aravamudan, and G. V. S. Rao, Prog. Solid State Chem. **15**, 55 (1983).
[12] L. Minervini, R. W. Grimes, and K. E. Sickafus, J. Am. Ceram. Soc. **83**, 1873 (2000).
[13] R. D. Shannon, Acta Crystallogr., Sect. A: Cryst. Phys., Diffr., Theor. Gen. Ctystallogr. **32**, 751 (1976).
[14] D. E. P. Vanpoucke, P. Bultinck, S. Cottenier, V. Van Speybroeck, and I. Van Driessche, Phys. Rev. B **84**, 054110 (2011).
[15] V. F. Sears, Neutron News **3**, 29 (1992).
[16] F. Brisse and O. Knop, Can. J. Chem. **45**, 609 (1967).
[17] H. J. Koo, M. H. Whangbo, and B. J. Kennedy, J. Solid State Chem. **136**, 269 (1998).
[18] K. D. Liss, B. Hunter, M. Hagen, T. Noakes, and S. Kennedy, Physica B **385-386**, 1010 (2006).
[19] K. S. Wallwork, B. J. Kennedy, and D. Wang, in *The High Resolution Powder Diffraction Beamline for the Australian Synchrotron*, edited by Jae-Young Choi and Seungyu Rah, AIP Conf. Proc. No. 879 (AIP, New York, 2007), pp. 879–882.

[20]B. A. Hunter and C. J. Howard, *RIETICA. A Computer Program for Rietveld Analysis of X-Ray and Neutron Powder Diffraction Patterns* (ANSTO, Lucas Heights Sydney, 1998).
[21]T. E. Dann, S. C. Chung, L. J. Huang, J. M. Juang, C. I. Chen, and K. L. Tsang, J. Synchrotron Radiat. **5**, 664 (1998).
[22]R. Clements, J. R. Hester, B. J. Kennedy, C. D. Ling, and A. P. J. Stampfl, J. Solid State Chem. **184**, 2108 (2011).
[23]M. Yashima, S. Kobayashi, and T. Yasui, Solid State Ionics **177**, 211 (2006).
[24]M. J. Verkerk, G. M. H. Vandevelde, A. J. Burggraaf, and R. B. Helmholdt, J. Phys. Chem. Solids **43**, 1129 (1982).
[25]C. H. Lee, H. Oyanagi, C. Sekine, I. Shirotani, and M. Ishii, Phys. Rev. B **60**, 13253 (1999).
[26]Z. M. Zhang, B. J. Kennedy, C. J. Howard, L.-Y. Jang, K. S. Knight, M. Matsuda, and M. Miyake, J. Phys.: Condens. Matter **22**, 445401 (2010).
[27]A. Kotani, K. O. Kvashnina, S. M. Butorin, and P. Glatzel, J. Electron Spectrosc. Relat. Phenom. **184**, 210 (2011).
[28]P. Nachimuthu, W. C. Shih, R. S. Liu, L. Y. Jang, and J. M. Chen, J. Solid State Chem. **149**, 408 (2000).
[29]A. V. Soldatov, T. S. Ivanchenko, S. Della Longa, A. Kotani, Y. Iwamoto, and A. Bianconi, Phys. Rev. B **50**, 5074 (1994).
[30]Z. Zeng, M. Greenblatt, and M. Croft, Phys. Rev. B **63**, 224410 (2001).
[31]S. Garcia-Martin, M. A. Alario-Franco, D. P. Fagg, and J. T. S. Irvine, J. Mater. Chem. **15**, 1903 (2005).
[32]J. W. Wang, F. X. Zhang, J. Lian, R. C. Ewing, and U. Becker, Acta Mater. **59**, 1607 (2011).
[33]M. Lang, F. X. Zhang, J. M. Zhang, J. W. Wang, B. Schuster, C. Trautmann, R. Neumann, U. Becker, and R. C. Ewing, Nature Mater. **8**, 793 (2009).